

# An Overview of PET Radiochemistry, Part 1: The Covalent Labels $^{18}\text{F}$ , $^{11}\text{C}$ , and $^{13}\text{N}$

Verena Pichler<sup>1</sup>, Neydher Berroterán-Infante<sup>1</sup>, Cecile Philippe<sup>1</sup>, Chrysoula Vraka<sup>1</sup>, Eva-Maria Klebermass<sup>1</sup>, Theresa Balber<sup>1</sup>, Sarah Pfaff<sup>1</sup>, Lukas Nics<sup>1</sup>, Markus Mitterhauser<sup>1,2</sup>, and Wolfgang Wadsak<sup>1,3</sup>

<sup>1</sup>Division of Nuclear Medicine, Department of Biomedical Imaging and Image-Guided Therapy, Medical University of Vienna, Vienna, Austria; <sup>2</sup>Ludwig Boltzmann Institute Applied Diagnostics, Vienna, Austria; and <sup>3</sup>CBmed - Center for Biomarker Research in Medicine, Graz, Austria

**Learning Objectives:** On successful completion of this activity, participants should be able to (1) identify the most important PET tracers currently applied in clinical routine and research; (2) illustrate the overall process of radiochemical production, from cyclotron production to quality control; and (3) classify the generally applied PET tracers according to their mode of action.

**Financial Disclosure:** The authors of this article have indicated no relevant relationships that could be perceived as a real or apparent conflict of interest.

**CME Credit:** SNMMI is accredited by the Accreditation Council for Continuing Medical Education (ACCME) to sponsor continuing education for physicians. SNMMI designates each *JNM* continuing education article for a maximum of 2.0 AMA PRA Category 1 Credits. Physicians should claim only credit commensurate with the extent of their participation in the activity. For CE credit, SAM, and other credit types, participants can access this activity through the SNMMI website (<http://www.snmmilearningcenter.org>) through September 2021.

This continuing educational article introduces the radiochemistry of PET tracers that exhibit a covalently bound radiolabel with the nuclides  $^{11}\text{C}$ ,  $^{13}\text{N}$ , and  $^{18}\text{F}$ . The overall process of PET tracer production is explained, starting from the production of the radionuclide in a cyclotron; followed by the automatization process of the radiosynthesis, including the necessary steps for the respective synthesis; and finalized with the requirements for quality control.

**J Nucl Med 2018; 59:1350–1354**

DOI: 10.2967/jnumed.117.190793

**T**he accessibility of molecular imaging probes for PET is built on 3 major pillars: radionuclide production, methodology for radiolabeling, and techniques for radiotracer production.

It is essential to deeply understand the molecular behavior of the imaging probes (radiotracers) and the underlying (patho-) physiology and interaction with the molecular target. Quantifiable signals in PET are directly related to the radionuclide bound to the imaging probe's backbone. These signals are directly involved in molecular processes and therefore enable a direct *in vivo* readout of the extent of pathophysiologic changes or biodistribution within the organism (1,2).

It is pivotal to use a commonly recognized and precise (radio-) chemical language leading to a recently harmonized tracer nomenclature within the radiopharmaceutical community (3).

The aim of this article is to consolidate the basic principles of the most important radiotracers comprising a covalent PET radiolabel (i.e.,  $^{18}\text{F}$ ,  $^{11}\text{C}$ , and  $^{13}\text{N}$ ).

## RADIONUCLIDE PRODUCTION

After 80 y, the message “The cyclotron evidently proves to be a sort of hen laying golden eggs” (Fig. 1), written by Emilio Segré to Ernest Lawrence (4), after the discovery of technetium from a residual molybdenum strip of the first cyclotron developed by Lawrence, is still valid. Indeed, a cyclotron is the only source of most PET radionuclides, including  $^{11}\text{C}$ ,  $^{13}\text{N}$ , and  $^{18}\text{F}$ . Accordingly, our golden radionuclides are respectively produced in a cyclotron by irradiation of  $^{14}\text{N}$ ,  $^{16}\text{O}$ , and  $^{18}\text{O}$  with low- and medium-energy (10–20 MeV) protons ( $\text{H}^+$ ), obtained after the acceleration of negative hydride ions ( $\text{H}^-$ ) by means of an electric field in a growing spiral path due to the presence of a magnetic field. After reaching the desired energy, the beam of accelerated negative ions passes a thin foil of graphite, which strips the electrons of the hydride ions, thus producing the desired protons. The resulting protons are then directed to bombard a target filled with the appropriate material, where the irradiation and consequently the nuclear reaction take place (5).

1.  $^{11}\text{C}$  production ( $^{14}\text{N}(\text{p},\alpha)^{11}\text{C}$ ) involves the use of a gas target filled with nitrogen ( $^{14}\text{N}_2$ ), which is mixed with trace amounts of oxygen or hydrogen to obtain  $[^{11}\text{C}]\text{CO}_2$  or  $[^{11}\text{C}]\text{CH}_4$ , respectively, which are further used to label the desired molecule.

2.  $^{13}\text{N}$  ( $^{16}\text{O}(\text{p},\alpha)^{13}\text{N}$ ) is generally obtained from liquid water ( $[^{16}\text{O}]\text{H}_2\text{O}$ ).

3.  $^{18}\text{F}$  can be produced via 2 methods; the first one uses highly enriched  $[^{18}\text{O}]\text{H}_2\text{O}$  as target material, and  $^{18}\text{O}(\text{p},\text{n})^{18}\text{F}$  to yield  $[^{18}\text{F}]\text{F}^-$ ; whereas the second requires a gas target filled with  $^{20}\text{Ne}$  to achieve  $[^{18}\text{F}]\text{F}_2$  gas. For the  $[^{18}\text{F}]\text{F}_2$  production, the target is bombarded with deuterons ( $^2\text{H}^+$ ) instead of protons ( $^{20}\text{Ne}(\text{d},\alpha)^{18}\text{F}$ ).

However,  $^{11}\text{C}$  synthesis often involves a posttarget synthesis to transform the relatively unreactive building blocks  $[^{11}\text{C}]\text{CO}_2$  and  $[^{11}\text{C}]\text{CH}_4$  to more reactive species, such as  $[^{11}\text{C}]\text{CH}_3\text{I}$  among others. This transformation can be conducted either via a wet procedure or via a gas-phase process.

## AUTOMATION PROCESS

The production of radiotracers has become an important issue in nuclear medicine. Synthesis time has a major influence for

Received Dec. 27, 2017; revision accepted Jul. 16, 2018.  
For correspondence or reprints contact: Wolfgang Wadsak, Medical University of Vienna, Waehringer Guertel 18-20, A-1090 Vienna, Austria.  
E-mail: [wolfgang.wadsak@meduniwien.ac.at](mailto:wolfgang.wadsak@meduniwien.ac.at)  
Published online Jul. 24, 2018.  
COPYRIGHT © 2018 by the Society of Nuclear Medicine and Molecular Imaging.



**FIGURE 1.** Nuclear reactions of golden radionuclides.

counteracting losses due to natural decay and radiation protection. Therefore, the production of radiotracers is preferentially accomplished using a fully automated synthesizer, which should provide easy handling. Most commonly used systems are conventional heaters with reusable reaction vessels or a single-use cassette-based system. The latter one can be equipped with a new cassette for every batch and offers the possibility to modify the chemical form of the active species (e.g., concentration or purification). Single-use cassettes are applied for routinely produced tracers such as [ $^{18}\text{F}$ ]FDG. Unfortunately, these systems are not available for demanding labeling procedures or newly developed compounds, and consequently, in these cases the conventional vessel-based module is used. Additionally, this kind of synthesizer is favorable for optimization or establishment of new techniques.

In some cases, conventional heating systems are not sufficient for successful radiolabeling. Therefore, rarely used techniques such as microwave heating or microfluidic systems are advantageous. In contrast to conventional heaters, microwaves heat a solution uniformly, which accelerates the reaction rate and subsequently facilitates successful product formation. Microfluidic systems are designed for working with small volumes (nanoliter range) and channel sizes in micrometers. Both methods offer the opportunity to heat a reaction mixture over its boiling point due to enhanced pressure causing a better conversion. Several radiotracers have already been successfully produced using these techniques (6–8), for example, [ $^{18}\text{F}$ ]FDG and [ $^{18}\text{F}$ ]fluoroethylcholine.

### QUALITY CONTROL AND REGULATIONS

Every radiotracer for diagnosis has to be prepared on the day of application because of the short half-life of the respective radionuclide ( $^{18}\text{F}$ , 110 min;  $^{11}\text{C}$ , 20 min; and  $^{13}\text{N}$ , 10 min), and therefore the quality of the applied radiotracer must be carefully examined before patient administration. Quality control guidelines are embedded in the monographs for radiopharmaceutical products (9). There are a variety of different laws, statutory guidelines, and regulations regarding the correct handling, production, and quality control in the course of a preparation process. They are defined in the medicinal laws of every country.

The obligatory quality control parameters for intravenous application of radiotracers are as follows: physical parameters (osmolality, pH, and visual appearance); radionuclidic purity ( $\gamma$ -spectrum, calculation of half-life); radiochemical purity (radioactive by-products); determination of molar activity and chemical purity; solvent residues; and microbial contamination (sterility, bacterial endotoxins).

Safe and robust chromatographic methods should be used to keep the time frame for quality control as short as possible and therefore the resulting activity as well as the molar activity high (1,10,11).

### [ $^{18}\text{F}$ ]FDG

The glucose analog [ $^{18}\text{F}$ ]FDG (2-[ $^{18}\text{F}$ ]fluoro-2-deoxy-D-glucose; Fig. 2) is undoubtedly the most successful PET tracer, allowing the visualization of energy metabolism in cells. It takes advantage of the so-called Warburg effect, a metabolic shift toward aerobic glycolysis mostly seen in tumors or inflammatory cells, resulting in a higher demand for glucose (12). [ $^{18}\text{F}$ ]FDG is transported via glucose transporters and phosphorylated intracellularly like glucose, but unlike the latter, it cannot be introduced into the glycolytic pathway because of the  $^{18}\text{F}$  atom and is thus accumulated. This so-called trapping mechanism and a wide scope of applications ranging from various types of tumors to malignant changes in brain activity have paved the way for it to become the workhorse of PET. As alterations of glucose and hence [ $^{18}\text{F}$ ]FDG uptake do not reflect only pathologic processes but benign alterations as well, this tracer's versatility is its Achilles' heel at the same time (1).

The success story took its course in Brookhaven National Laboratory in 1976, where [ $^{18}\text{F}$ ]FDG was synthesized for the first time. In principle, [ $^{18}\text{F}$ ]FDG can be produced via either electrophilic addition or nucleophilic substitution. The former, original, synthesis route used the precursor 3,4,6-tri-*O*-acetyl-D-glucal as a source of a double bond to attack the electrophilic [ $^{18}\text{F}$ ]F $_2$  gas. This pathway, though, gave only a low yield of around 8%, as the chemical reaction led to a mixture of radioactive and nonradioactive fluorine-substituted mannose and glucose. Different electrophilic agents such as acetylhypofluorite failed to improve the [ $^{18}\text{F}$ ]FDG production, leading to the implementation of the generally higher-yielding nucleophilic approach using [ $^{18}\text{F}$ ]fluoride ions. Nowadays, the prevailing synthesis route shown in Figure 3 uses aliphatic nucleophilic substitution with [ $^{18}\text{F}$ ]fluoride against the triflate-leaving group of the precursor 1,3,4,6-tetra-*O*-acetyl-2-*O*-trifluoromethanesulfonyl- $\beta$ -D-mannopyranose (mannose triflate) in the presence of the phase transfer catalyst Kryptofix 222 (Merck). The other hydroxyl groups are protected with acetyl groups throughout the synthesis, which must be removed, usually with base or acid, to yield [ $^{18}\text{F}$ ]FDG up to 70%–80% (13,14).

Today, [ $^{18}\text{F}$ ]FDG synthesis is fully automated, making high yields and reproducibility feasible. In addition, [ $^{18}\text{F}$ ]FDG can potentially be produced only once per day for all patients and even allows distribution to other PET centers because of the relatively long half-life of  $^{18}\text{F}$ .

### AMINO ACIDS AND DERIVATIVES

The continuous glucose utilization by the human brain hampers [ $^{18}\text{F}$ ]FDG PET imaging strategies for brain tumor imaging. Consequently, radiolabeled amino acids (AAs) are broadly applied in brain PET imaging because of their low uptake in healthy brain (15,16).

The most common nuclides for labeling AAs are  $^{11}\text{C}$  and  $^{18}\text{F}$ , with the first nuclide enabling an unaltered structure of the AA and the second one allowing application in PET centers without on-site production. Additionally, the desired radiolabeled AA should be composed of more than 95% of the naturally occurring L-form, as the D-AA has no biologic function.

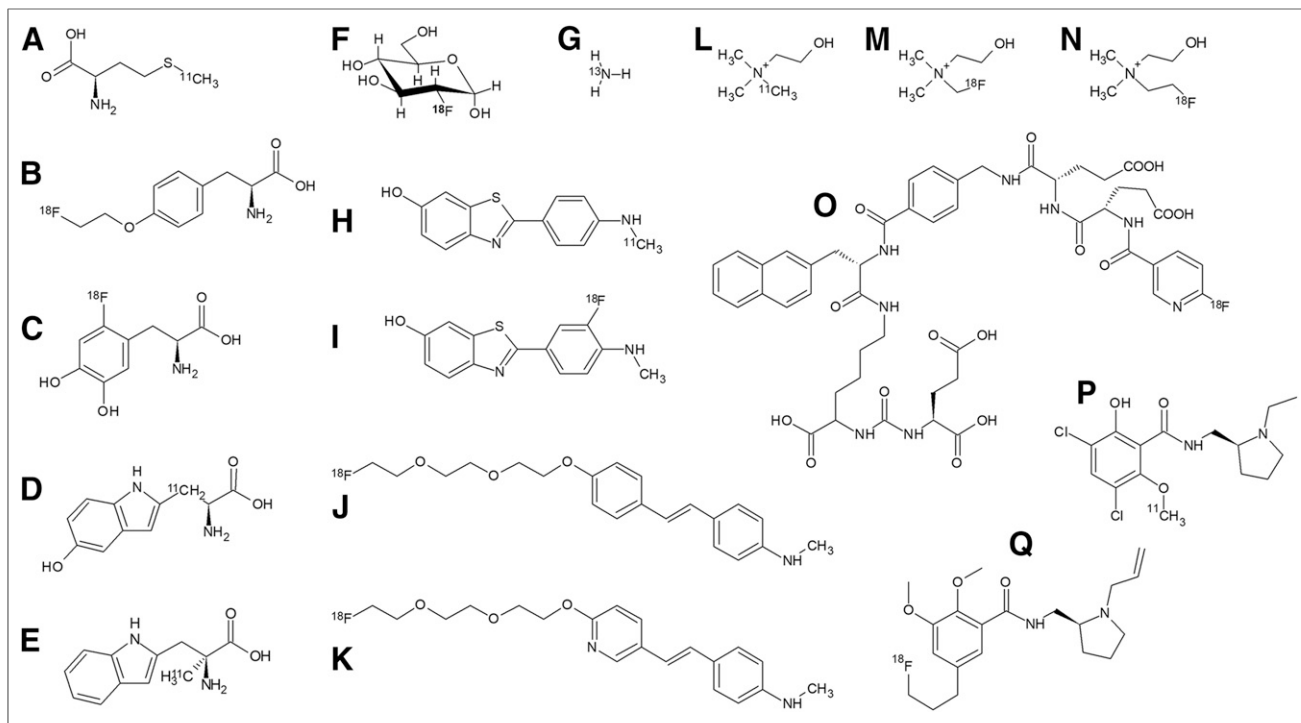


**FIGURE 2.** Overview on different PET tracers with covalent radiolabel: [ $^{11}\text{C}$ ]methionine (A), *O*-(2-[ $^{18}\text{F}$ ]fluoroethyl)-L-tyrosine (B), 3,4-dihydroxy-6-[ $^{18}\text{F}$ ]fluoro-L-phenylalanine (C), 5-hydroxy-L- $[\beta\text{-}^{11}\text{C}]$ tryptophan (D),  $\alpha$ -[ $^{11}\text{C}$ ]methyltryptophan (E), [ $^{18}\text{F}$ ]FDG (F), [ $^{13}\text{N}$ ]NH $_3$  (G), [ $^{11}\text{C}$ ]PIB (H), [ $^{18}\text{F}$ ]flutemetamol (I), [ $^{18}\text{F}$ ]florbetaben (J), [ $^{18}\text{F}$ ]florbetapir (K), [ $^{11}\text{C}$ ]choline (L), [ $^{18}\text{F}$ ]fluoromethylcholine (M), [ $^{18}\text{F}$ ]fluoroethylcholine (N), [ $^{18}\text{F}$ ]PSMA-1007 (O), [ $^{11}\text{C}$ ]raclopride (P), and [ $^{18}\text{F}$ ]fallypride (Q).

A popular radiolabeled AA so far is L-[methyl- $^{11}\text{C}$ ]methionine for brain tumor imaging, although its use is limited to a maximum of 2–3 patients per production, caused by the short half-life of  $^{11}\text{C}$ . [ $^{11}\text{C}$ ]methionine synthesis is mostly conducted with either L-homocysteine thiolactone hydrochloride or L-homocysteine as precursor. Accordingly, [ $^{11}\text{C}$ ]CH $_3\text{I}$  is introduced into a mixture of the respective precursor and a base. Purification takes place either via solid-phase extraction or reversed-phase high-performance liquid chromatography (HPLC). The reaction allows a great variety of solvents, such as ethanol/water, acetone/water, or acetonitrile (17,18). Other precursor/synthetic routes described in

the literature were not applicable for routine production because of their complexity or safety issues.

*O*-(2-[ $^{18}\text{F}$ ]fluoroethyl)-L-tyrosine ([ $^{18}\text{F}$ ]FET) displays similar uptake and image contrast to L-[methyl- $^{11}\text{C}$ ]methionine (19) but is advantageous because of the half-life of  $^{18}\text{F}$ . [ $^{18}\text{F}$ ]FET is not metabolized and not incorporated into protein biosynthesis but is transported via tumor cell-specific transport, which is accelerated in malignant cells, leading to high accumulation in tumor tissue. [ $^{18}\text{F}$ ]FET was initially synthesized in a 2-step reaction consisting of [ $^{18}\text{F}$ ]fluorination of ethylene glycol-1,2-ditosylate and subsequent [ $^{18}\text{F}$ ]fluoroethylation of an L-tyrosine salt including HPLC purification twice (20). An efficient routine production was presented starting from *O*-(2-tosyloxyethyl)-*N*-trityl-L-tyrosine tert-butyl ester as a precursor (1-pot reaction) (21). The procedure comprises subsequent acidic deprotection and HPLC purification. Another approach uses 2-bromoethyl triflate as a precursor, whereby the intermediate ([ $^{18}\text{F}$ ]bromofluoroethane) is subsequently distilled, requiring a synthesis module with 2 reactors. Favorably, HPLC purification is not needed and purification can be accomplished using simple solid-phase extraction (22). Moreover, an Ni(II) complex of a (*S*)-tyrosine Schiff base was presented as an enantiomerically pure labeling precursor for [ $^{18}\text{F}$ ]FET (23).

The nonproteinogenic AA 3,4-dihydroxy-6-[ $^{18}\text{F}$ ]fluoro-L-phenylalanine ([ $^{18}\text{F}$ ]FDOPA) reflects the presynaptic dopaminergic synthesis and the enzyme activity of the aromatic AA decarboxylase. [ $^{18}\text{F}$ ]FDOPA finds broad application in neuropsychiatric diseases, headed by Parkinson disease, motion disorders, and schizophrenia. Moreover, its application spectrum expanded to brain tumor imaging and peripheral tumor imaging, whereby [ $^{18}\text{F}$ ]FDOPA reflects the upregulation of AA transport in malignant tissue as a consequence of increased proliferation. Nucleophilic

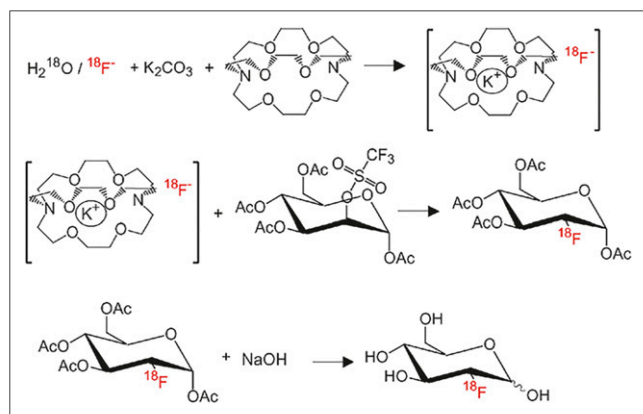


**FIGURE 3.** Synthetic scheme of [ $^{18}\text{F}$ ]FDG radiosynthesis via nucleophilic substitution.

radiofluorination approaches provide [<sup>18</sup>F]FDOPA in high chemical yields and with high molar activities. The introduction of fluoride-18 was either conducted using an enantiomerically pure precursor followed by deprotection and purification or was introduced in an achiral precursor, which necessitates chiral phase-transfer catalysts to yield the enantioselective product (24,25). Moreover, copper-mediated nucleophilic radiofluorination of the protected L-3,4-dihydroxyphenylalanine stannane was reported previously (26).

Currently applied PET tracers for investigating serotonin synthesis are the tryptophan derivatives  $\alpha$ -[<sup>11</sup>C]methyltryptophan ([<sup>11</sup>C]AMT) and 5-hydroxy-L-[<sup>11</sup>C]tryptophan. The radiosyntheses for both tracers are quite complex and have multiple steps.  $\alpha$ -[<sup>11</sup>C]methyltryptophan is prepared by deprotonation of the respective precursor with a strong base, mostly lithium diisopropyl amine, at low temperature (−55°C–75°C). Subsequently, [<sup>11</sup>C]CH<sub>3</sub>I is introduced into the solution, and after acidic and basic deprotection the final product is obtained via purification with C18 solid-phase extraction (27,28). The less applied 5-hydroxy-L-[<sup>11</sup>C]tryptophan is synthesized via an enzymatic reaction (29). Recently, <sup>18</sup>F analogs of tryptophan were described enabling distribution of the tracers (30,31).

### CHOLINE DERIVATIVES

Considering the high impact of prostate cancer in the world, several PET tracers have been developed to image this malignancy in vivo (32). Choline, an essential molecule for the biosynthesis of cell membrane phospholipids, has accordingly been labeled with <sup>11</sup>C as well as <sup>18</sup>F (e.g., [<sup>18</sup>F]fluoromethylcholine and [<sup>18</sup>F]fluoroethylcholine) to target prostate cancer as well as brain tumors. Although other tracers, such as [<sup>68</sup>Ga]prostate-specific membrane antigen (PSMA)-11, [<sup>18</sup>F]PSMA-1007 and [<sup>18</sup>F]DCFBC (*N*-[*N*-[(*S*)-1,3-dicarboxypropyl]carbamoyl]-4-[<sup>18</sup>F]fluorobenzyl-L-cysteine), have shown superior results in first trials, choline derivatives are still the most clinically used PET tracer for prostate cancer.

The synthesis of the radiolabeled choline derivatives is as follows. For [<sup>11</sup>C]choline, the reactive species [<sup>11</sup>C]methyl iodide reacts with a solution of dimethylaminoethanol in dimethylformamide to give the product, which is purified and formulated with physiologic saline. For [<sup>18</sup>F]fluoromethylcholine, [<sup>18</sup>F]F<sup>−</sup> is dried until no traces of water are present; posteriorly, dibromomethane is used to produce the labeled building block, [<sup>18</sup>F]bromofluoromethane, which after distillation, reacts with dimethylaminoethanol to yield the product [<sup>18</sup>F]fluoromethylcholine. For [<sup>18</sup>F]fluoroethylcholine, radiosynthesis proceeds similarly to [<sup>18</sup>F]fluoromethylcholine; however, bromoethyltriflate is added instead of dibromomethane to obtain the labeled compound [<sup>18</sup>F]bromofluoroethane. Another method uses ethylene ditosylate to afford the labeled building block 2-[<sup>18</sup>F]fluoroethyl tosylate. Purification of all these tracers is straightforward because of the cationic nature of the product, which allows isolation of the product with a cation exchange resin.

### [<sup>13</sup>N]NH<sub>3</sub>

The radionuclide <sup>13</sup>N is widely applied as [<sup>13</sup>N]NH<sub>3</sub> (<sup>13</sup>N]ammonia) for evaluating myocardial perfusion. Production of [<sup>13</sup>N]NH<sub>3</sub> requires a cyclotron on-site and a fast synthesis procedure because of the short half-life of 10.0 min. High amounts of <sup>13</sup>N can be produced by irradiation of water ([<sup>16</sup>O]H<sub>2</sub>O) with protons (5). Depending on the proton energy, radiolysis in the presence of

oxygen generates the by-products [<sup>13</sup>N]nitrite and [<sup>13</sup>N]nitrate. These side products must be reduced with a catalyst, namely the Devarda alloy, in alkaline solution, yielding 50%–90% [<sup>13</sup>N]NH<sub>3</sub> (33,34).

### RADIOLIGANDS TARGETING SPECIFIC PROTEINS

Besides the aforementioned PET tracers, which image biologic or physiologic functions (e.g., L-[methyl-<sup>11</sup>C]methionine and [<sup>18</sup>F]FDG for metabolism and [<sup>13</sup>N]NH<sub>3</sub> for perfusion), a plethora of tracers that directly target specific receptors, transporters, enzymes, and antigens is used in clinical routine, trials, or preclinical studies.

In oncology, PSMA is of peculiar and current relevance. The expression of PSMA is upregulated in prostate cancer and prostate metastases and can be target by the radiolabeled peptide [<sup>18</sup>F]PSMA-1007. The latest data indicate high tumor-to-background ratios with excellent pharmacokinetic properties and, therefore, suitable imaging of midget tumors and metastases. Specific PET tracers in oncology, as [<sup>18</sup>F]PSMA-1007, enable early diagnosis and are an adjuvant in the planning of the ideal treatment (35).

Receptors can be targeted, either by antagonists (inhibitor of receptor activity) or agonists (activator of signal transduction), to image the density or the change in expression of specific targets (e.g., receptors). The basic principle is the comparison of imaging data between healthy controls and patients, measuring the expression levels before and after a specific treatment, or targeting a specific receptor that is upregulated in tumors. Additionally, specific radiolabeled substrates can provide insight into the functionality of transporters. The representation of receptors is a major request of clinical research targeting brain function. Plenty of radiotracers with different targets (e.g., dopaminergic system) have been developed, with the goal of determining pathophysiologic changes in brain diseases, ascertaining new therapeutic approaches, and determining therapeutic effects. Among others, [<sup>11</sup>C]raclopride and [<sup>18</sup>F]fallypride are especially efficient in reflecting the D<sub>2</sub>/D<sub>3</sub> subtype or extrapyramidal D<sub>3</sub> receptor, respectively, (36).

### PET TRACERS FOR AMYLOID- $\beta$ PLAQUES

Besides the presence of intracellular neurofibrillary tangles, extracellular amyloid plaques in the gray matter are a pathologic hallmark of Alzheimer disease (37). Several PET tracers have been developed to visualize the fibrillary amyloid- $\beta$  plaques in vivo.

[<sup>11</sup>C]Pittsburgh compound B ([<sup>11</sup>C]PIB) (2-[4-(methylamino)phenyl]-1,3-benzothiazol-6-ol) was the first PET tracer for specific amyloid- $\beta$  plaque imaging. It is a thioflavin-T analog, a fluorescent dye used to stain amyloid plaques in vitro. The radiosynthesis consists of a direct <sup>11</sup>C-methylation of the aniline moiety of the unprotected precursor 2-(4'-aminophenyl)-6-hydroxybenzothiazole (38). Subsequent purification takes place via reversed-phase-HPLC (39). For widespread clinical use, <sup>18</sup>F-labeled amyloid tracers have been introduced, allowing distribution from a production site to multiple PET centers.

[<sup>18</sup>F]flutemetamol (Vizamyl; GE Healthcare) is a fluoroderivative of [<sup>11</sup>C]Pittsburgh compound B (40). The 2 other <sup>18</sup>F-labeled amyloid tracers, [<sup>18</sup>F]florbetaben (Neuraceq; Piramal) and [<sup>18</sup>F]florbetapir (AMYViD; Eli Lilly) (41–43), are derived from stilbene. They are synthesized by direct [<sup>18</sup>F]fluorination via nucleophilic substitution of the respective N-Boc protected tosylate precursor. To remove the N-Boc-protecting group, aqueous HCl is added after the reaction. All 3 <sup>18</sup>F-labeled tracers are purified by reversed-phase-HPLC.

## CONCLUSION

The versatility and applicability of covalently bound radionuclides are enormous, especially as the chemical structure is not altered ( $^{11}\text{C}$ ) or only slightly altered ( $^{18}\text{F}$ ) compared with PET tracers with a metal-based radiolabel. Limitations are mainly due to the time factor and equipment, such as a cyclotron on-site, to facilitate supplies from the production site to the PET centers.

## REFERENCES

1. Wadsak W, Mitterhauser M. Basics and principles of radiopharmaceuticals for PET/CT. *Eur J Radiol*. 2010;73:461–469.
2. Mitterhauser M, Wadsak W. Imaging biomarkers or biomarker imaging? *Pharmaceuticals (Basel)*. 2014;7:765–778.
3. Coenen HH, Gee AD, Adam M, et al. Consensus nomenclature rules for radiopharmaceutical chemistry: setting the record straight. *Nucl Med Biol*. 2017;55:v–xi.
4. Heilbron J, Seidel R. *Lawrence and His Laboratory: A History of the Lawrence Berkeley Laboratory*. Vol I. Berkeley, CA: University of California Press; 1989:367.
5. Qaim SM, Clark JC, Crouzel C, et al. PET radionuclide production. In: Stöcklin G, Pike VW, eds. *Radiopharmaceuticals for Positron Emission Tomography*. New York, NY: Springer; 1993:1–43.
6. Lee C-C, Sui G, Elizarov A, et al. Multistep synthesis of a radiolabeled imaging probe using integrated microfluidics. *Science*. 2005;310:1793–1796.
7. Pascali G, Nannavecchia G, Pitzianti S, Salvadori PA. Dose-on-demand of diverse  $^{18}\text{F}$ -fluorocholine derivatives through a two-step microfluidic approach. *Nucl Med Biol*. 2011;38:637–644.
8. Philippe C, Ungersboeck J, Schirmer E, et al. [ $^{18}\text{F}$ ]FE@SNAP: a new PET tracer for the melanin concentrating hormone receptor 1 (MCHR1)—microfluidic and vessel-based approaches. *Bioorg Med Chem*. 2012;20:5936–5940.
9. European Pharmacopoeia Commission. *European Pharmacopoeia*. 6th ed. Strasbourg, France: Council of Europe. 2007:1167–1173.
10. Nics L, Steiner B, Klebermass E-M, et al. Speed matters to raise molar radioactivity: fast HPLC shortens the quality control of C-11 PET-tracers. *Nucl Med Biol*. 2018;57:28–33.
11. Passchier J. Fast high performance liquid chromatography in PET quality control and metabolite analysis. *Q J Nucl Med Mol Imaging*. 2009;53:411–416.
12. Potter M, Newport E, Morten KJ. The Warburg effect: 80 years on. *Biochem Soc Trans*. 2016;44:1499–1505.
13. Hamacher K, Coenen HH, Stöcklin G. Synthesis D-glucose using aminopolyether supported nucleophilic substitution. *J Nucl Med*. 1986;27:235–238.
14. Ido T, Wan C-N, Casella V, et al. Labeled 2-deoxy-D-glucose analogs:  $^{18}\text{F}$ -labeled 2-deoxy-2-fluoro-D-glucose, 2-deoxy-2-fluoro-D-mannose and  $^{14}\text{C}$ -2-deoxy-2-fluoro-D-glucose. *J Labelled Comp Radiopharm*. 1978;14:175–183.
15. Crippa F, Alessi A, Serafini GL. PET with radiolabeled aminoacids. *Q J Nucl Med Mol Imaging*. 2012;56:151–162.
16. Qi Y, Liu X, Li J, Yao H, Yuan S. Fluorine-18 labeled amino acids for tumor PET/CT imaging. *Oncotarget*. 2017;8:60581–60588.
17. Bolster JM, Vaalburg W, Elsinga PH, Wynberg H, Woldring MG. Synthesis of DL-[1- $^{11}\text{C}$ ]methionine. *Int J Rad Appl Instrum [A]*. 1986;37:1069–1070.
18. Långström B, Lundqvist H. The preparation of  $^{11}\text{C}$ -methyl iodide and its use in the synthesis of  $^{11}\text{C}$ -methyl-L-methionine. *Int J Appl Radiat Isot*. 1976;27:357–363.
19. Weber WA, Wester HJ, Grosu AL, et al. O-(2-[ $^{18}\text{F}$ ]fluoroethyl)-L-tyrosine and L-[methyl- $^{11}\text{C}$ ]methionine uptake in brain tumours: initial results of a comparative study. *Eur J Nucl Med*. 2000;27:542–549.
20. Wester HJ, Herz M, Weber W, et al. Synthesis and radiopharmacology of O-(2-fluoroethyl)-L-tyrosine for tumor imaging. *J Nucl Med*. 1999;40:205–212.
21. Hamacher K, Coenen HH. Efficient routine production of the  $^{18}\text{F}$ -labelled amino acid O-(2-[ $^{18}\text{F}$ ]fluoroethyl)-L-tyrosine. *Appl Radiat Isot*. 2002;57:853–856.
22. Zuhayra M, Alfteimi A, Von Forstner C, Lützen U, Meller B, Henze E. New approach for the synthesis of [ $^{18}\text{F}$ ]fluoroethyltyrosine for cancer imaging: simple, fast, and high yielding automated synthesis. *Bioorg Med Chem*. 2009;17:7441–7448.
23. Krasikova RN, Kuznetsova OF, Fedorova OS, Maleev VI, Saveleva TF, Belokon YN. No carrier added synthesis of O-(2'-[ $^{18}\text{F}$ ]fluoroethyl)-L-tyrosine via a novel type of chiral enantiomerically pure precursor, NiII complex of a (S)-tyrosine Schiff base. *Bioorg Med Chem*. 2008;16:4994–5003.
24. Pretze M, Wängler C, Wängler B. 6-[ $^{18}\text{F}$ ]fluoro-L-DOPA: a well-established neurotracer with expanding application spectrum and strongly improved radio-syntheses. *Biomed Res Int*. 2014;2014:674063.
25. Visser AKD, Van Waarde A, Willemsen ATM, et al. Measuring serotonin synthesis: from conventional methods to PET tracers and their (pre)clinical implications. *Eur J Nucl Med Mol Imaging*. 2011;38:576–591.
26. Makaravage KJ, Brooks AF, Mossine AV, Sanford MS, Scott PJ. Copper-mediated radiofluorination of arylstannanes with [ $^{18}\text{F}$ ]KF. *Org Lett*. 2016;18:5440–5443.
27. Chakraborty PK, Mangner TJ, Chugani DC, Muzik O, Chuguni H. A high-yield and simplified procedure for the synthesis of [ $^{11}\text{C}$ ]methyl-L-tryptophan. *Nucl Med Biol*. 1996;23:1005–1008.
28. Huang X, Xiao X, Gillies RJ, Tian H. Design and automated production of  $^{11}\text{C}$ -alpha-methyl-L-tryptophan ( $^{11}\text{C}$ -AMT). *Nucl Med Biol*. 2016;43:303–308.
29. Bjurling P, Antoni G, Watanabe Y, Långström B. Enzymatic synthesis of carboxy- $^{11}\text{C}$ -labelled L-tyrosine, L-DOPA, L-tryptophan and 5-hydroxy-L-tryptophan. *Acta Chem Scand*. 1990;44:178–182.
30. Chiotellis A, Muller A, Mu L, et al. Synthesis and biological evaluation of  $^{18}\text{F}$ -labeled fluoroethoxy tryptophan analogues as potential PET tumor imaging agents. *Mol Pharm*. 2014;11:3839–3851.
31. Giglio B, Fei H, Wang M, et al. Synthesis of 5-[ $^{18}\text{F}$ ]fluoro- $\alpha$ -methyl tryptophan: new trp based PET agents. *Theranostics*. 2017;7:1524–1530.
32. Evans JD, Jethwa KR, Ost P, et al. Prostate cancer-specific PET radiotracers: a review on the clinical utility in recurrent disease. *Pract Radiat Oncol*. 2018;8:28–39.
33. Maddahi J, Packard RRS. Cardiac PET perfusion tracers: current status and future directions. *Semin Nucl Med*. 2014;44:333–343.
34. Korsakov MV, Krasikova RN, Fedorova OS. Production of high yield [ $^{13}\text{N}$ ] ammonia by proton irradiation from pressurized aqueous solutions. *J Radioanal Nucl Chem*. 1996;204:231–239.
35. Giesel FL, Hadaschik B, Cardinale J, et al. F-18 labelled PSMA-1007: biodistribution, radiation dosimetry and histopathological validation of tumor lesions in prostate cancer patients. *Eur J Nucl Med Mol Imaging*. 2017;44:678–688.
36. Elsinga PH, Hatano K, Ishiwate K. PET tracers for imaging of the dopaminergic system. *Curr Med Chem*. 2006;13:2139–2153.
37. Tiraboschi P, Hansen LA, Thal LJ, Corey-Bloom J. The importance of neuritic plaques and tangles to the development and evolution of AD. *Neurology*. 2004;62:1984–1989.
38. Mathis CA, Wang Y, Holt DP, Huang GF, Debnath ML, Klunk WE. Synthesis and evaluation of  $^{11}\text{C}$ -labeled 6-substituted 2-arylbenzothiazoles as amyloid imaging agents. *J Med Chem*. 2003;46:2740–2754.
39. Wilson AA, Garcia A, Chestakova A, Kung H, Houle S. A rapid one-step radiosynthesis of the  $\beta$ -amyloid imaging radiotracer N-methyl-[ $^{11}\text{C}$ ]2-(4'-methylaminophenyl)-6-hydroxybenzothiazole ([ $^{11}\text{C}$ ]-6-OH-BTA-1). *J Labelled Comp Radiopharm*. 2004;47:679–682.
40. Philippe C, Haeusler D, Mitterhauser M, et al. Optimization of the radiosynthesis of the Alzheimer tracer 2-(4-N-[ $^{11}\text{C}$ ]methylaminophenyl)-6-hydroxybenzothiazole ([ $^{11}\text{C}$ ]PIB). *Appl Radiat Isot*. 2011;69:1212–1217.
41. Koole M, Lewis DM, Buckley C, et al. Whole-body biodistribution and radiation dosimetry of  $^{18}\text{F}$ -GE067: a radioligand for in vivo brain amyloid imaging. *J Nucl Med*. 2009;50:818–822.
42. Zhang W, Oya S, Kung MP, Hou C, Maier DL, Kung HF. F-18 polyethylene-glycol stilbenes as PET imaging agents targeting A $\beta$  aggregates in the brain. *Nucl Med Biol*. 2005;32:799–809.
43. Carpenter AP, Pontecorvo MJ, Hefti FF, Skovronsky DM. The use of the exploratory IND in the evaluation and development of  $^{18}\text{F}$ -PET radiopharmaceuticals for amyloid imaging in the brain: a review of one company's experience. *Q J Nucl Med Mol Imaging*. 2009;53:387–393.